

# mTOR-dependent stimulation of the association of eIF4G and eIF3 by insulin

Thurl E Harris<sup>1</sup>, An Chi<sup>2</sup>, Jeffrey Shabanowitz<sup>2</sup>, Donald F Hunt<sup>2</sup>, Robert E Rhoads<sup>3</sup> and John C Lawrence Jr<sup>1,\*</sup>

<sup>1</sup>Department of Pharmacology, University of Virginia, Charlottesville, VA, USA, <sup>2</sup>Department of Chemistry, University of Virginia, Charlottesville, VA, USA and <sup>3</sup>Department of Biochemistry and Molecular Biology, Louisiana State University Health Sciences Center, Shreveport, LA, USA

**Insulin stimulates protein synthesis by increasing translation initiation. This response is mediated by mTOR and is believed to result from 4EBP1 phosphorylation, which allows eIF4E to bind eIF4G. Here, we present evidence that mTOR interacts directly with eIF3 and that mTOR controls the association of eIF3 and eIF4G. Activating mTOR signaling with insulin increased by as much as five-fold the amount of eIF4G bound to eIF3. This novel effect was blocked by rapamycin and other inhibitors of mTOR, and it required neither eIF4E binding to eIF4G nor eIF3 binding to the 40S ribosomal subunit. The increase in eIF4G associated with eIF3 occurred rapidly and at physiological concentrations of insulin. Moreover, the magnitude of the response was similar to the increase in eIF4E binding to eIF4G produced by insulin. Thus, increasing eIF4G association with eIF3 represents a potentially important mechanism by which insulin, as well as amino acids and growth factors that activate mTOR, stimulate translation.**

*The EMBO Journal* (2006) 25, 1659–1668. doi:10.1038/sj.emboj.7601047; Published online 16 March 2006

**Subject Categories:** signal transduction; proteins

**Keywords:** eIF4E; 4EBP1; eIF4B; mRNA translation initiation; rapamycin

## Introduction

Insulin stimulates protein synthesis in a wide variety of cell types, both *in vivo* and *in vitro* (Kimball *et al*, 1994). This response involves an increase in the rate of initiation, which is generally the limiting phase of mRNA translation. Included in initiation are recognition of the capped mRNA by initiation factors, melting of secondary structure in the 5' UTR, and binding of the small ribosomal subunit (Hershey and Merrick, 2000; Preiss and Hentze, 2003). The initial processes depend on eIF4F, a complex of eIF4G, eIF4E, and eIF4A (Gingras *et al*, 1999). eIF4E binds the mRNA cap

(m<sup>7</sup>GpppN, where N is any nucleotide), thus directing eIF4F to begin at the 5' end of the message. eIF4A is a helicase that unwinds mRNA to facilitate binding and/or scanning by the 40S ribosomal subunit. eIF4B enhances the helicase activity of eIF4A, although eIF4B has not been shown to physically associate with eIF4A or eIF4G (Preiss and Hentze, 2003). eIF4G binds both eIF4E and eIF4A, as well as several other proteins, including eIF3, polyA binding protein (PABP), and the protein kinase, Mnk (Gingras *et al*, 1999; Keiper *et al*, 1999). The binding of eIF4G to eIF3 connects eIF4F to the 43S complex, which contains the 40S ribosomal subunit, GTP-eIF2<sup>-Met</sup>tRNA<sub>i</sub>, eIF3, eIF1, eIF1A, and eIF5. This positions the small ribosomal subunit at the 5'-end of the message, setting the stage for scanning and selection of the correct start codon.

The best characterized mechanism through which insulin stimulates translation initiation involves the eIF4E binding protein, 4EBP1 (Gingras *et al*, 1999; Harris and Lawrence Jr, 2003). Hypophosphorylated 4EBP1 binds tightly to eIF4E, and it represses cap-dependent translation by blocking the binding of eIF4G to eIF4E. The eIF4E binding motif in 4EBP1 (YxxxxLΦ, where x is any amino acid and Φ is an aliphatic amino acid, most often L) is also found in eIF4G (Mader *et al*, 1995). Introducing LΦ to AA mutations in either 4EBP1 or eIF4G abolishes high-affinity binding to eIF4E. Insulin increases the phosphorylation of 4EBP1 in multiple sites, including T36 and T45 (Harris and Lawrence, 2003). This triggers dissociation of the 4EBP1–eIF4E complex, allowing eIF4E to engage eIF4G. The effect of insulin on 4EBP1 phosphorylation is markedly attenuated by rapamycin (Lin *et al*, 1995). eIF4G is also phosphorylated in a rapamycin-sensitive manner (Raught *et al*, 2000), although the role of eIF4G phosphorylation is unclear.

Sensitivity to rapamycin is indicative of a process controlled by mTORC1, one of two mTOR signaling complexes (Martin and Hall, 2005; Sarbassov *et al*, 2005). mTORC1 contains mTOR, the G protein β homolog, mLst8 (also known as GβL), and the substrate-binding subunit, raptor (Martin and Hall, 2005; Sarbassov *et al*, 2005). The best characterized targets of mTORC1 are 4EBP1 and S6K1 (Harris and Lawrence, 2003). Raptor binds to these targets via the TOS motif, which is formed by the five COOH terminal amino acids (FEMDI) in 4EBP1, and amino acids 5–9 in S6K-1 (FDIDL) (Nojima *et al*, 2003; Schalm *et al*, 2003).

eIF3 is the largest and one of the most complex initiation factors (Hershey and Merrick, 2000). Mammalian eIF3 contains 12 subunits designated eIF3a–eIF3k, in order of decreasing size (from 166 500 to 25 100) (Browning *et al*, 2001). eIF3 binds the 40S ribosomal subunit, both blocking premature binding of the 60S subunits and enhancing binding of ternary complex (GTP–eIF2<sup>-Met</sup>tRNA<sub>i</sub>). Studies in *Saccharomyces cerevisiae* indicate that eIF3a, eIF3b, eIF3c, eIF3g and eIF3i form an essential core, with the other subunits serving regulatory roles (Asano *et al*, 1998). Several eIF3 subunits have been implicated in RNA binding and/or in interactions with other

\*Corresponding author. Department of Pharmacology, University of Virginia Health System, PO Box 800735, 1300 Jefferson Park Avenue, Charlottesville, VA 22908-0735, USA. Tel.: +1 434 924 1584; Fax: +1 434 982 3575; E-mail: jcl3p@virginia.edu

Received: 19 January 2006; accepted: 22 February 2006; published online: 16 March 2006

initiation factors. For example, eIF3d and eIF3g bind RNA (Nygard and Westermann, 1982; Bandyopadhyay and Maitra, 1999), eIF3a interacts with eIF4B (Vornlocher *et al*, 1999), and eIF3c binds eIF5 (Phan *et al*, 1998). Although the eIF3 subunit that binds eIF4G has not been identified, the connection between eIF4G and eIF3 is critical for initiation, since it connects the eIF4G-associated factors to the 43S preinitiation complex (Hershey and Merrick, 2000).

The present study was prompted by a yeast two-hybrid screen in which an interaction was detected between eIF3f and a fusion protein containing a region of mTOR. In investigating the possible control of eIF3 by mTOR, insulin was found to produce a dramatic, rapamycin-sensitive, increase in the association of eIF4G and eIF3. Results of experiments investigating this novel and potentially important mechanism for the control of translation initiation are presented.

## Results

### Evidence of an interaction between eIF3f and mTOR

Stringent screening of a 3T3-L1 adipocyte yeast two-hybrid library with bait containing a COOH terminal fragment of mTOR (CTmTOR) yielded three hits: a protein similar to ubiquitin-specific protease 34 (XP\_483996), a hypothetical single-strand nucleotide-binding protein (XP\_127811), and eIF3f. XP\_483996 and XP\_127811 were not pursued. To investigate the interaction between eIF3f and mTOR, we determined whether HA-eIF3f that had been overexpressed in 293T cells could be captured *in vitro* by using GST-CTmTOR bound to GSH agarose (Figure 1A). As a control we also assessed retention of HA-eIF3f by a resin prepared by binding GST to GSH agarose. After incubating the two resins with cell extracts, the samples were washed and the bound proteins were subjected to SDS-PAGE. The amount of

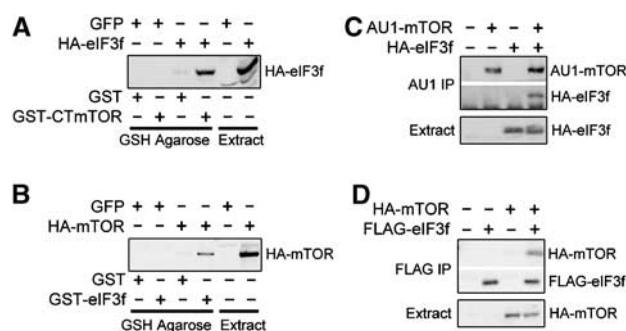


**Figure 1** Evidence of an interaction between eIF3f and mTOR. Extracts (750  $\mu$ l) of 293T cells overexpressing epitope tagged forms of mTOR and eIF3f proteins were incubated with affinity resins or antibodies as described below. After washing resins or immune complexes, the bound proteins were eluted and subjected to SDS-PAGE, along with extract samples (15  $\mu$ l). Immunoblots were then prepared to detect the epitope tagged proteins. (A) Extracts from cells overexpressing GFP or HA-tagged eIF3f were incubated with GSH-beads (15  $\mu$ l) bound to either GST (2  $\mu$ g) or GST-CTmTOR (2  $\mu$ g). (B) Extracts from 293T cells overexpressing GFP (as a control) or HA-tagged mTOR were incubated with GSH-beads (15  $\mu$ l) bound to either GST (2  $\mu$ g) or GST-eIF3f (2  $\mu$ g). (C) AU1-tagged mTOR and/or HA-tagged eIF3f were overexpressed in 293T cells before immunoprecipitations were conducted with AU1 antibodies. The band appearing just below HA-eIF3f in the AU1 IP is the heavy chain of the AU1 antibody. (D) HA-tagged mTOR and/or FLAG tagged eIF3f were overexpressed before conducting immunoprecipitations with FLAG antibodies.

HA-eIF3f recovered with the mTOR affinity resin was much greater than that retained by the GST resin (Figure 1A), indicative of an interaction between the mTOR fragment and eIF3f. Similarly, full-length HA-tagged mTOR that had been overexpressed in 293T cells could be captured by incubating extracts with a GST-eIF3f affinity resin (Figure 1B). Next, we determined whether an association could be detected between epitope-tagged forms of mTOR and eIF3f that had been overexpressed in 293T cells. HA-eIF3f coimmunoprecipitated with AU1-mTOR (Figure 1C), and HA-mTOR coimmunoprecipitated with FLAG-eIF3f (Figure 1D). Thus, results from yeast two-hybrid screening, affinity purifications with eIF3f and mTOR resins, and reciprocal coimmunoprecipitations of epitope-tagged proteins support the conclusion that mTOR binds eIF3f. These results also suggested that mTOR might control the function of eIF3.

### Insulin promotes the association of eIF3 and eIF4G in a rapamycin-sensitive manner

To search for effects of mTOR on eIF3, the initiation factor was immunoprecipitated from extracts of untreated 3T3-L1 adipocytes or cells that had been incubated with insulin to activate mTOR signaling. Samples were then subjected to SDS-PAGE and proteins were stained with silver or Coomassie blue (Figure 2A). eIF3a and eIF3b, and several other eIF3 subunits (not shown), were detected, although eIF3a stained poorly with silver. Insulin did not change the amount of eIF3a or eIF3b that immunoprecipitated; however, the hormone markedly increased the amount of a  $M_r \approx 220$  000 protein, initially designated 220K. The effect of insulin was abolished by rapamycin, indicating that the association was dependent on mTOR. To identify 220K, a gel slice containing the protein from insulin-treated cells was excised. 220K was digested with trypsin, and 18 of the resulting peptides were sequenced (Figure 2B). All 18 sequences matched exactly sequences in mouse eIF4G-1.

In analyzing the eIF4G-1 peptides, two new phosphorylation sites were identified (LLNGAP-pS<sup>413</sup>-PPAVDL and KAA-pS<sup>1204</sup>-LTGDR, where pS denotes the phosphorylated residue) (Figure 2B). Based on numbering of previously identified sites (Raught *et al*, 2000), S413 and S1204 correspond to S369 and S1170. Whether these two new sites are controlled by insulin is not known.

To confirm that insulin stimulated the association of eIF4G with eIF3, immunoprecipitations were conducted using antibodies to either eIF3b or eIF4G, and immunoblots were prepared with antibodies to the three eIF4F subunits and to three of the eIF3 subunits (Figure 2C). eIF4G was readily detected in immune complexes isolated with eIF3b antibodies, as were eIF4A and eIF4E. The eIF3 and eIF4F subunits were not detected in nonimmune complexes, supporting the specificity of the immunoprecipitation. Insulin increased by several fold the coimmunoprecipitation of all three eIF4F subunits with eIF3b, and the effects of insulin were abolished by rapamycin. Similarly, insulin increased in a rapamycin-sensitive manner the amounts of eIF3a, eIF3b and eIF3i that coimmunoprecipitated with eIF4G.

The reciprocal coimmunoprecipitation of eIF4G and eIF3 was confirmed in insulin dose-response experiments (Figure 3A). The maximum effect of insulin represented a five-fold increase in eIF4G associated with eIF3 (Figure 3B). The half-maximum response occurred at 10  $\mu$ U/ml (70 pM).

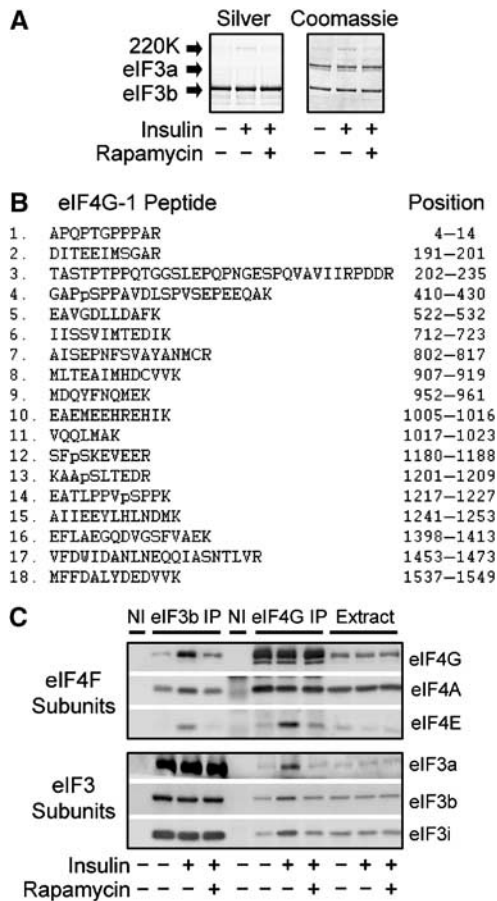


**Figure 2** Identification of eIF4G-1 as a protein that associates with eIF3 in a rapamycin-sensitive manner in response to insulin. 3T3-L1 adipocytes were incubated at 37°C without or with 20 nM rapamycin for 1 h. After adding insulin as indicated, the incubations were continued for 15 min. (A) eIF3 was immunoprecipitated by using antibodies to eIF3b. After thoroughly washing immune complexes, samples were subjected to SDS-PAGE. Proteins were stained with either silver or Coomassie blue. Regions of the gels surrounding eIF3a (which stained very poorly with silver) and eIF3b are shown. The 220K band contains a protein (apparent  $M_r = 220,000$ ) whose abundance increases in response to insulin. (B) A gel slice containing 220K was incubated with trypsin and the resulting peptides were eluted and analyzed by tandem mass spectrometry. Sequences of 18 tryptic peptides were matched to the protein sequence of mouse eIF4G-1 (NP\_001005331.1). pS denotes phosphorylated S, which was found in four of the peptides. (C) Extract samples (750  $\mu$ l) were incubated with protein G-agarose beads to which nonimmune IgG (NI), eIF3b antibodies (eIF3b IP), or eIF4G antibodies (eIF4G IP) had been bound. Immune complexes were washed before immunoprecipitated proteins and extract samples (15  $\mu$ l) were subjected to SDS-PAGE. Immunoblots of eIF4G, eIF4A, eIF4E, eIF3a, eIF3b, and eIF3i are presented.

This concentration falls well within the range of circulating insulin concentrations *in vivo*, and it is comparable to the concentration producing half-maximal activation of glucose transport in adipocytes (Simpson and Cushman, 1986), a classic response to the hormone.

Rapamycin potently inhibited the stimulatory effect of insulin on increasing eIF4G binding to eIF3 (Figure 3C). The half-maximum response to rapamycin occurred at 0.4 nM (Figure 3D), which is very near the concentration that half maximally inhibits the activation of S6K in adipocytes (Lin and Lawrence Jr, 1997). To inhibit mTOR rapamycin must first bind to the intracellular protein, FKBP12

(Abraham and Wiederrecht, 1996). FK506 binds to the same site in FKBP12 as rapamycin, but the FK506-FKBP12 complex does not inhibit mTOR. Consequently, FK506 acts as a competitive inhibitor of those effects of rapamycin that result from inhibition of mTOR signaling. Incubating adipocytes with FK506 was without effect on eIF4G binding to eIF3, in either the absence or presence of insulin (Figure 3E). However, FK506 abolished the inhibitory effect of rapamycin on the association of the two initiation factors. As expected, FK506 attenuated the inhibitory effects of rapamycin on other processes known to be mediated by mTOR, including, the phosphorylation of 4EBP1, eIF4G and S6K1.

**eIF4E binding to eIF4G is not required for the enhancement of eIF3-eIF4G association by insulin**

The amounts of eIF3a, eIF3b and eIF3i coimmunoprecipitating with eIF4G changed in parallel in response to insulin and rapamycin (Figure 2C), consistent with the expected behavior of the three proteins as subunits of the eIF3 complex. In contrast, the relative amount of eIF4E coimmunoprecipitating with eIF3 was increased more by insulin than the amounts of either eIF4G or eIF4A (Figure 2C, Supplementary Figure S1). The preferential increase in eIF4E can be explained by the effect of insulin on increasing eIF4E bound to eIF4G, as evidenced by the marked insulin-stimulated increase in eIF4E found in eIF4G immunoprecipitates (Figure 2C).

Since the effects of insulin on eIF4G binding to both eIF3 and eIF4E were rapamycin-sensitive, experiments were conducted to determine whether binding of eIF4E to eIF4G was responsible for enhancing the interaction between eIF4G and eIF3. An LL to AA mutation was introduced into the eIF4E binding site of eIF4G. HA-tagged forms of wild type, and mutant eIF4G proteins were then overexpressed along with FLAG-tagged eIF4E in 293T cells. The interaction between wild-type eIF4G and eIF4E was readily detected by using  $m^7$ GTP-agarose to capture eIF4G-eIF4E complexes (Figure 4A) or by coimmunoprecipitating FLAG-eIF4E (Figure 4B). In contrast, binding of the mutant eIF4G to eIF4E was not detected, confirming that the mutation in the eIF4E binding site disrupted the high-affinity interaction between eIF4G and eIF4E. Next, HA-tagged forms of wild type and mutant eIF4G proteins were overexpressed in 3T3-L1 adipocytes by using adenoviruses, and extracts were prepared after incubating cells with insulin and or rapamycin. Both HA-eIF4G proteins coimmunoprecipitated with endogenous eIF3 (Figure 4C). Moreover, the coimmunoprecipitation of both was stimulated by insulin in a rapamycin-sensitive manner (Figure 4D). Thus, enhancement of eIF3-eIF4G association by insulin does not appear to occur secondarily to binding of eIF4E to eIF4G.

**eIF3 binding to the small ribosomal subunit is not required for the enhancement of eIF3-eIF4G association by insulin**

Binding of eIF3 to the 40S ribosomal subunit was evident from the coimmunoprecipitation of ribosomal protein S6 (rpS6) and eIF3 (Figure 5A). Neither insulin nor rapamycin changed the amount of rpS6 that coimmunoprecipitated with eIF3 (Figure 5B), indicating that the effect of insulin on eIF3 and eIF4G did not occur secondarily to an increase in the association of eIF3 with the small ribosomal subunit. To investigate the possibility that the effects of insulin on

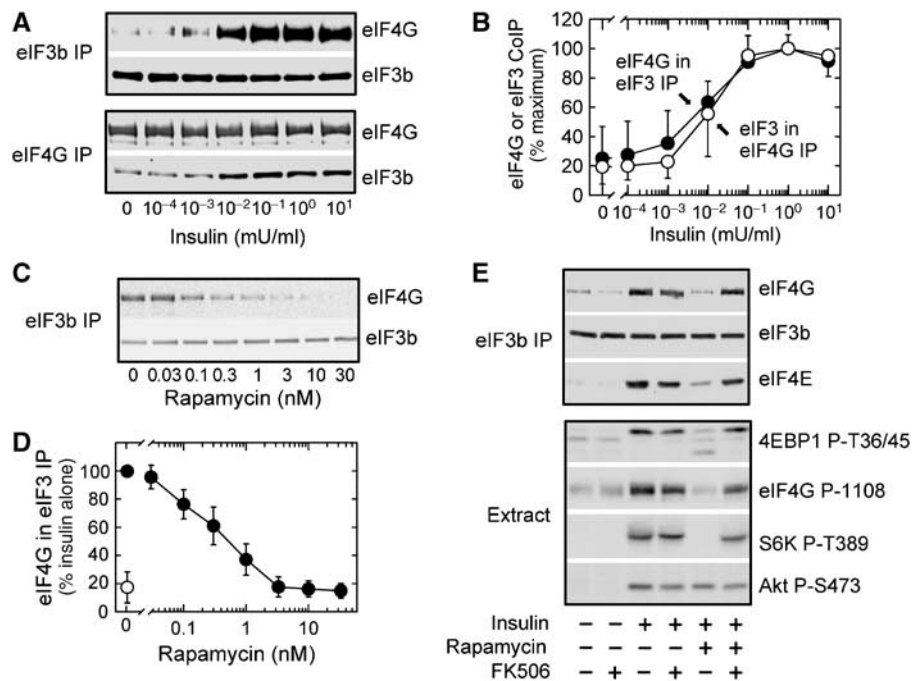


**Figure 3** Effects of insulin and rapamycin on eIF4G–eIF3 association. (A) Adipocytes were incubated with increasing concentrations of insulin for 15 min. Immune complexes were isolated after incubating extract samples (750  $\mu$ l) with either eIF3b antibodies (eIF3b IP) or eIF4G antibodies (eIF4G IP). The immunoprecipitated proteins were subjected to SDS–PAGE, and eIF4G and eIF3b immunoblots were prepared. (B) eIF4G and eIF3b that coimmunoprecipitated (CoIP) were expressed relative to the respective maximum amounts recovered. The results are mean values ( $\pm$  s.e.) from three experiments. (C) Adipocytes were incubated with increasing concentrations of rapamycin for 1 h, and then incubated with insulin (10 mU/ml) for 15 min. Immunoblots depict eIF4G and eIF3b recovered in immune complexes isolated using eIF3b antibodies. (D) The amounts of eIF4G that CoIP with eIF3 were expressed as percentages of the eIF4G recovered from cells incubated with insulin alone. The open symbol ( $\circ$ ) represents results from cells incubated without insulin or rapamycin. Mean values  $\pm$  s.e. of three experiments are presented. (E) Adipocytes were incubated without or with 2 nM rapamycin and/or 20  $\mu$ M FK506 for 1 h. Insulin (10 mU/ml) was then added as indicated, and the incubations were continued for 15 min. Immunoprecipitations were conducted with eIF3b antibodies, and immunoblots were prepared to detect the eIF4G, eIF3b, and eIF4E recovered. Immunoblots of extract samples were prepared with phosphospecific antibodies to sites in 4EBP1, eIF4G, Akt, and S6K1.

eIF3–eIF4G required eIF3 to be bound to the 40S subunit, initiation factors were extracted from ribosomal pellets by using high salt (Figure 5A). No rpS6 coimmunoprecipitated with eIF3 in the high salt extract, demonstrating that this fraction of eIF3 was free of 40S ribosomes. The effect of insulin on increasing eIF4G association with eIF3 was clearly retained in this ribosome-free fraction.

An effect of insulin on eIF4G association with eIF3 was also retained in the salt-washed ribosomal fraction (Figure 5A), indicating that binding to the small ribosomal subunit does not preclude the stimulatory effect of insulin on eIF4G–eIF3 association. Indeed, the effect of insulin on eIF4G–eIF3 presumably serves to enhance joining of eIF4F and the 43S initiation complex. Consistent with this view, we have found that insulin increases the amount of rpS6 that coimmunoprecipitates with eIF4G (results not shown). The total amount of eIF4G recovered with eIF3 was reduced by the high salt treatment (Figure 5A). Thus, the eIF3–eIF4G interaction may be somewhat destabilized by high salt.

As another approach to obtain eIF3 complexes free of the 40S ribosomal subunit, extract samples were fractionated by sucrose gradient centrifugation (Figure 5C). Most of the eIF3 appeared earlier in the gradient than the small ribosomal subunit, whose position was determined by measuring absorbance at 254 nm and by immunoblotting rpS6. Insulin clearly increased eIF4G associated with the eIF3 located in the ribosome-free fractions of the gradient.

### Insulin promotes dissociation of eIF4B from eIF3 in 3T3-L1 adipocytes

One hypothesis is that insulin enhances the association of eIF4G to eIF3 by promoting dissociation of an inhibitory factor from eIF3. To attempt to identify such a factor, proteins that coimmunoprecipitated with eIF3 were subjected to SDS–PAGE (Figure 6A). Staining with silver revealed that a  $M_r \approx 80\,000$  protein was decreased in response to insulin. Mass spectrometric sequencing of peptides identified this protein as eIF4B (Figure 6B). eIF4B detected by immunoblotting had the same electrophoretic mobility as the silver-stained band, and treating cells with insulin decreased the amount of eIF4B that coimmunoprecipitated with eIF3 (Figure 6C).

To investigate the possible effect of eIF4B on eIF4G binding to eIF3, HA-tagged forms of eIF4B and eIF4G were overexpressed in 293T cells. HA-eIF4B was without effect on the amount of HA-eIF4G that coimmunoprecipitated with eIF3 (Figure 6D). Likewise, overexpressing HA-eIF4G did not affect the amount of HA-eIF4B bound to eIF3. Since S6K1 may control the function of eIF4B (Raught *et al*, 2004), we overexpressed HA-S6K1, both alone and in combination with HA-eIF4B. In neither case was an effect on the amount of eIF4G that coimmunoprecipitated with eIF3 observed. As expected, overexpressing S6K1 increased the phosphorylation of rpS6, as evidenced by the decrease in electrophoretic mobility of rpS6. Interestingly, the amount of eIF4B recovered

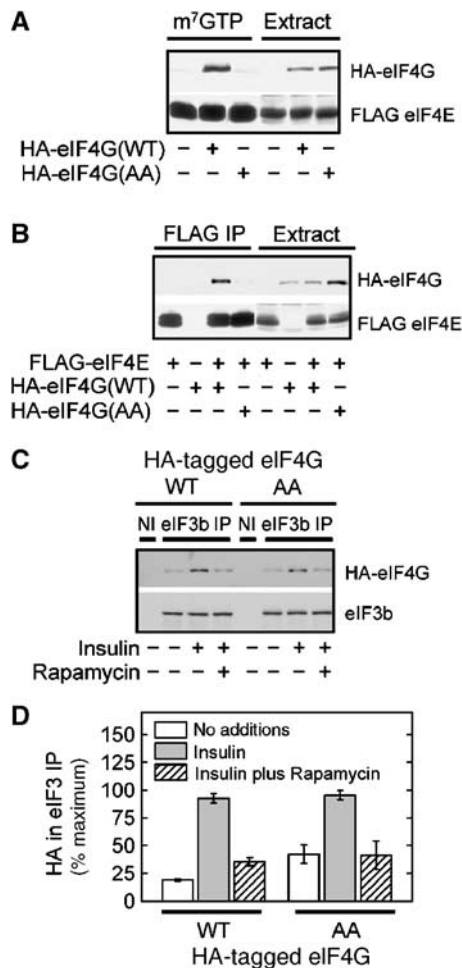


**Figure 4** The insulin-stimulated, rapamycin-sensitive, association of eIF4G with eIF3 does not require eIF4E binding to eIF4G. (A) FLAG-eIF4E was coexpressed in 293T cells with HA-tagged forms of either wild-type (WT) eIF4G or a mutant eIF4G (AA) rendered deficient in eIF4E binding. eIF4E was partially purified from extract samples (750  $\mu$ l) by using m<sup>7</sup>GTP agarose. Proteins were eluted from the beads and subjected to SDS-PAGE along with samples (15  $\mu$ l) of extract before immunoblots were prepared with antibodies to either the HA or FLAG epitopes. (B) Proteins were overexpressed as described above before immunoprecipitations were conducted with FLAG antibodies. Immunoblots were prepared with antibodies to either the HA or FLAG epitopes. (C) HA-tagged eIF4G (WT) and eIF4G (AA) were overexpressed in 3T3-L1 adipocytes by using adenoviral vectors. After 24 h, the cells were incubated without and with rapamycin and/or insulin as described above. Immunoprecipitations were conducted with nonimmune IgG or eIF3b antibodies. Immunoblots were prepared with eIF3b antibodies and antibodies to the HA epitope. (D) The relative amounts of HA-tagged forms of eIF4G that coimmunoprecipitated with eIF3 were expressed as percentages of the maximum HA signal recovered in each experiment. Mean values  $\pm$  s.e. from five experiments are presented.

with eIF3 was decreased by S6K1 overexpression. However, the failure of rapamycin to block the effect of insulin on eIF4B dissociation from eIF3 (Figure 6C) indicates that this insulin effect does not involve S6K1 activation, which is abolished by rapamycin. Moreover, the findings that eIF4B binding to eIF3 could be both increased by overexpression, and decreased by S6K1, without affecting the amount of eIF4G that coimmunoprecipitated with eIF3 does not support a key role of eIF4B in mediating the effect of insulin on eIF3 and eIF4G (Figure 6D).

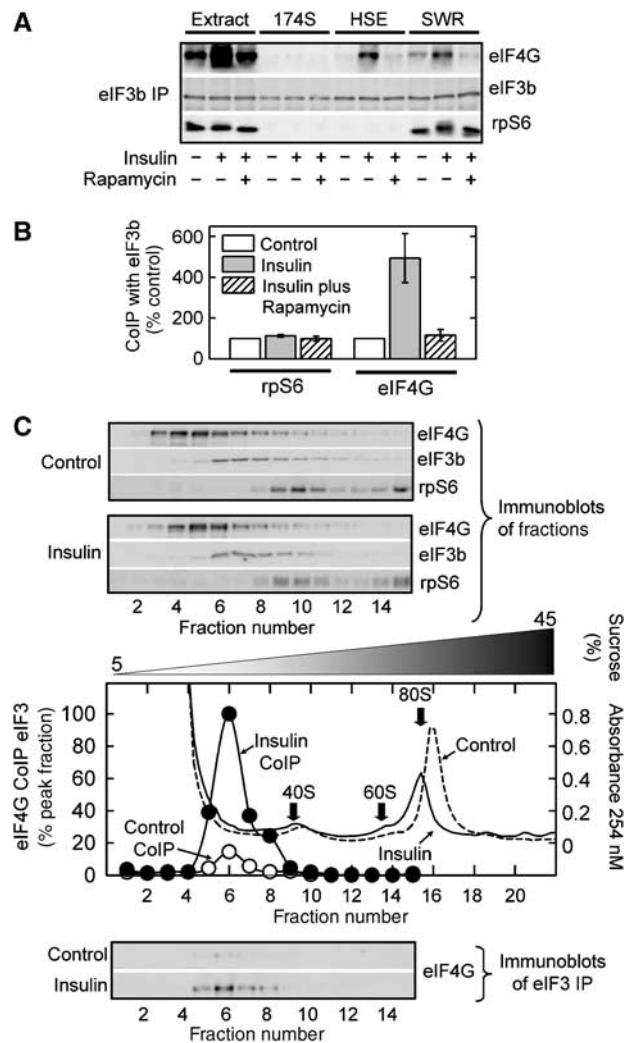


**Figure 5** The insulin-stimulated, rapamycin-sensitive, association of eIF4G with eIF3 does not require eIF3 to be bound to the small ribosomal subunit. Adipocytes were incubated without additions or with insulin and/or rapamycin as described in the legend to Figure 2. (A) Cells were homogenized in PSB, which contained 10 mM KCl, 1.3 mM magnesium acetate, 0.5 mM DTT, and 10 mM HEPES, pH 7.4 (Helentjaris and Ehrenfeld, 1978). The homogenates were centrifuged at 10000g for 10 min, and the supernatants (Extract) were removed. Samples of the extract were centrifuged at 174000g for 60 min. The resulting supernatants (174S) were collected, and the pellets were suspended in PSB plus 0.5 M KCl. After mixing at 4°C for 20 min, the suspensions were centrifuged at 174000g for 60 min. The supernatants (HSE) were collected and pellets (SWR) were suspended in PSB plus 0.1 M KCl. After adjusting the concentration of KCl in the Extract, 174S, and HSE fractions to 0.1 M, immunoprecipitations were conducted using eIF3b antibodies. Immunoblots show eIF4G, eIF3b and rpS6 recovered in the immune complexes. (B) Extracts were prepared as described in Materials and methods before immunoprecipitations were conducted using eIF3b antibodies. Results represent the relative amounts of rpS6 and eIF4G coimmunoprecipitating with eIF3 and are means  $\pm$  s.e. from five experiments. (C) Adipocyte extracts were layered on sucrose gradients and centrifuged. Immunoblots of eIF4G, eIF3b and rpS6 in fractions from the top of the gradient to the fraction containing 80S ribosomes, and immunoblots of eIF4G that coimmunoprecipitated with eIF3, are presented. The relative amounts of eIF4G coimmunoprecipitating with eIF3 from control (○) and insulin-treated (●) samples are plotted. Positions of the 40S, 60S and 80S ribosomes are indicated by the peaks of absorbance at 254 nm.

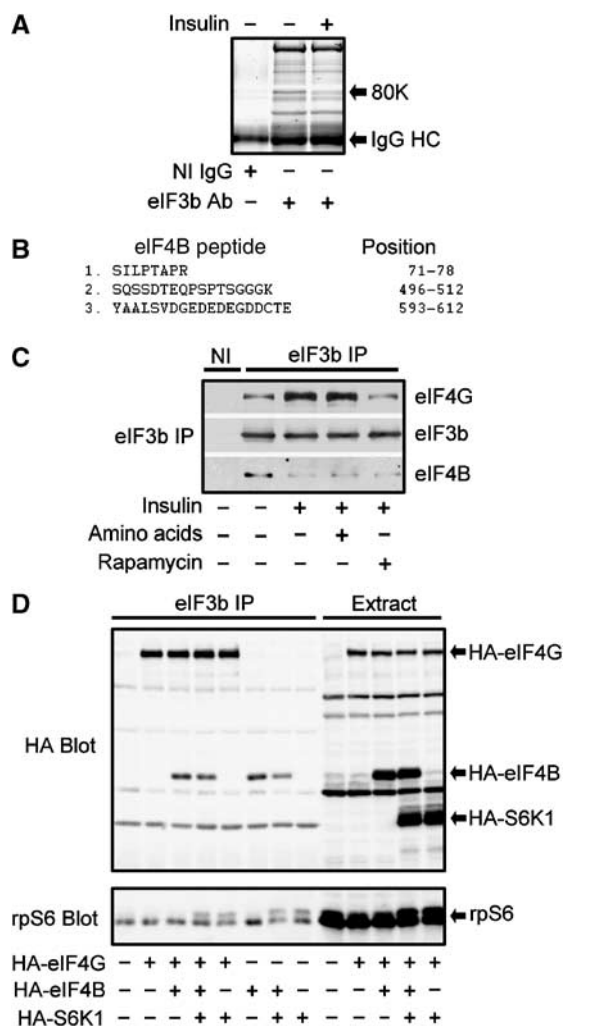


**Figure 6** Insulin-stimulated dissociation of eIF4B from the eIF3 complex. Adipocytes were incubated at 37°C without or with insulin for 15 min. (A) eIF3 was immunoprecipitated by using antibodies to eIF3b. The region of a silver-stained gel surrounding a protein (80K) that was decreased in response to insulin is shown. (B) A gel slice containing 80K was incubated with trypsin and the resulting peptides were analyzed by mass spectrometry. The sequences of three tryptic peptides unambiguously identifying 80K as mouse eIF4B (AK045250) are shown. (C) Adipocytes were incubated with additions as indicated for 15 min at 37°C. Amino acids were a combination of 2 × MEM mixture plus 0.5 mM leucine. Immunoblots of eIF4G, eIF3b, and eIF4B recovered after performing immunoprecipitations with nonimmune IgG (NI) or eIF3b antibodies are shown. (D) HA-tagged forms of eIF4G, eIF4B, and S6K1 were overexpressed in 293T cells. After immunoprecipitating eIF3 by using eIF3b antibodies, samples of the extracts and immunoprecipitated proteins were subjected to SDS-PAGE. An immunoblot showing HA-eIF4G, HA-eIF4B, and HA-S6K1 is presented, along with an immunoblot of rpS6.

#### Time course of insulin actions

A maximally effective concentration of insulin had little effect on the amount of eIF4G bound to eIF3 after 1 min of incubation (Figure 7A); however, the amount of eIF4G bound was increased more than two-fold after 3 min (Figure 7B). The response to insulin reached a stable plateau after 15 min. The decrease in eIF4B associated with eIF3 in response to insulin lagged behind the increase in eIF4G, again indicating that the dissociation of eIF4B is not responsible for increasing eIF4G–eIF3. Although insulin was without effect on the amount of ribosomal protein S6 that coimmunoprecipitated with eIF3,

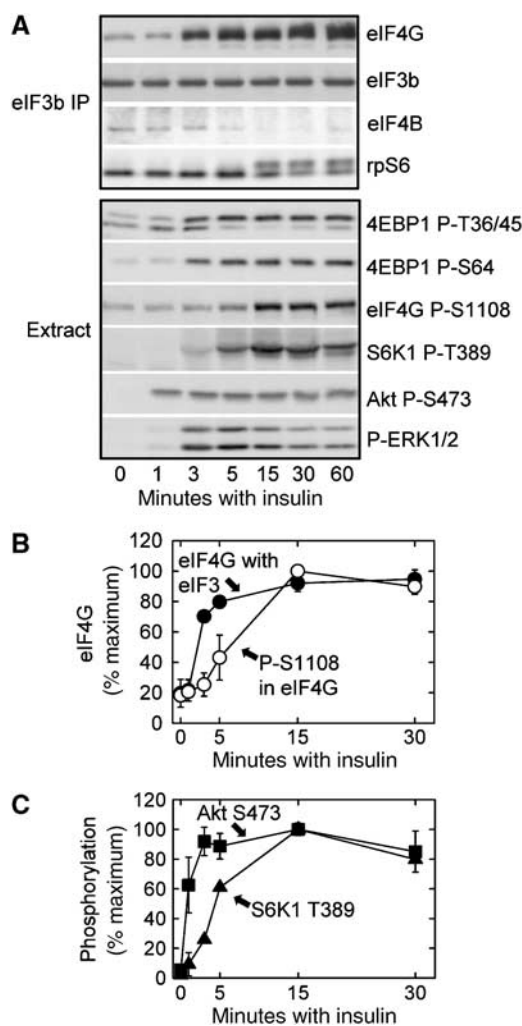


**Figure 7** Time courses of insulin responses. 3T3-L1 adipocytes were incubated for increasing times with a maximally effective concentration of insulin (10 mU/ml) before the cells were homogenized. (A) Immunoprecipitations were conducted using extracts (750 μl) and eIF3b antibodies. The immunoprecipitated proteins and extract samples (15 μl) were subjected to SDS-PAGE. Immunoblots were prepared to detect eIF4G, eIF3b, eIF4B, and ribosomal protein S6 (rpS6) that were recovered in the eIF3b immunoprecipitation (eIF3b IP). Phosphospecific antibodies were used to detect changes in phosphorylation of sites in 4EBP1, eIF4G, S6K1, Akt, and the ERK1 and ERK2 isoforms of MAP kinase. (B) The relative amounts of eIF4G that coimmunoprecipitated with eIF3, and the levels of phosphorylated Ser1108 in eIF4G, were determined. (C) The effects of insulin on the phosphorylation of S6K1 and Akt were assessed by immunoblotting with phosphospecific antibodies. The results in (B) and (C) are expressed relative to the respective maximum effects, and are mean values ± s.e. of three experiments. Error bars not shown fall within the symbols.

insulin did decrease the electrophoretic mobility of ribosomal protein S6 (rpS6), indicative of phosphorylation. However, the gel shift in rpS6 produced by insulin occurred more slowly than the increase in eIF4G binding to eIF3.

To allow comparison of the time course of the eIF3–eIF4G response to the phosphorylation of sites in other proteins, extract samples were immunoblotted with different phosphospecific antibodies (Figure 7A). The effect of insulin on eIF3–eIF4G bound to eIF3 (Figure 7B) occurred more rapidly than the phosphorylation of S6K1 (Figure 7C), but more slowly than the phosphorylation of S473 in Akt (Figure 7B and C).

In contrast to the phosphorylation of the Erk1 and Erk2 isoforms of MAP kinase, which peaked after 5 min and then markedly declined, the maximum stimulatory effect of insulin on eIF4G binding to eIF3 was maintained for at least 1 h (Figure 7A).

**eIF4G S1108 phosphorylation does not mediate insulin-stimulated eIF4G binding to eIF3**

The phosphorylation of S1108 in eIF4G lagged well behind the increase in binding of eIF4G to eIF3 (Figure 7B). Therefore, it seemed unlikely that the phosphorylation of S1108 was responsible for increasing the association of eIF4G with eIF3. To investigate further the role of S1108 phosphorylation, eIF3 immune complexes were incubated either without or with the catalytic subunit of protein phosphatase 1 $\alpha$  (PP1 $\alpha$ ). The phosphatase treatment completely dephosphorylated S1108, but it was without effect on eIF4G–eIF3 association, which was assessed by reciprocal coimmunoprecipitations with eIF3b or eIF4G antibodies (Supplementary Figure S1). Dephosphorylation of the site was also without effect on the amounts of eIF4E and eIF4A recovered with antibodies to either eIF3b or eIF4G.

**Effects of inhibitors and activators of signaling pathways on eIF4G binding to eIF3**

To investigate further the mechanisms involved in the insulin response, adipocytes were incubated with inhibitors of PI 3 kinase, mTOR, and MAP kinase signaling. The MAP kinase kinase inhibitor, U0126, was without effect on eIF4G binding to eIF3 (Figure 8A). Immunoblotting with phosphospecific antibodies to the activating sites in ERK1 and ERK2 confirmed that the inhibitor blocked activation of these two MAP kinase isoforms (results not shown). Incubating adipocytes with LY294002, wortmannin, or theophylline essentially abolished the stimulatory effect of insulin on binding of eIF4G to eIF3 (Figure 8B). Theophylline inhibits mTOR directly (Harris and Lawrence, 2003), presumably explaining the inhibitory effect of this methylxanthine on the association of eIF4G and eIF3. LY294002 and wortmannin are best known as inhibitors of PI 3 kinase, although both of these agents have the potential to inhibit mTOR catalytic activity (Brunn *et al*, 1996). Indeed, LY294002 is equally effective in inhibiting mTOR and PI 3 kinase. Consequently, inhibition of mTOR could account for the effects of this drug on eIF4G–eIF3 association. mTOR is less sensitive than PI 3 kinase to wortmannin, and the concentration of wortmannin in these experiments (100 nM) was sufficient to inhibit PI 3 kinase but not mTOR (Brunn *et al*, 1996). Therefore, the results with wortmannin are consistent with the hypothesis that PI 3 kinase is upstream in the signaling pathway mediating insulin action on eIF4G–eIF3 association.

The stimulation of eIF4G binding to eIF3 was not limited to insulin. Activation of mTOR signaling by amino acids produced significant stimulation (Figure 8D). Certain growth factors that activated mTOR signaling, as evidence by phosphorylation of S6K1, were also effective (Figure 8D). For example, both IGF-1 and PDGF increased eIF4G associated with eIF3, although the effect of PDGF was somewhat smaller than that of insulin. FGF-1 caused the most striking increase in MAP kinase phosphorylation (Figure 8C); however, FGF-1 did not increase the association of eIF4G and eIF3 (Figure 8D). Similarly, EGF and PMA promoted MAP kinase phosphorylation, but these agents were relatively ineffective in

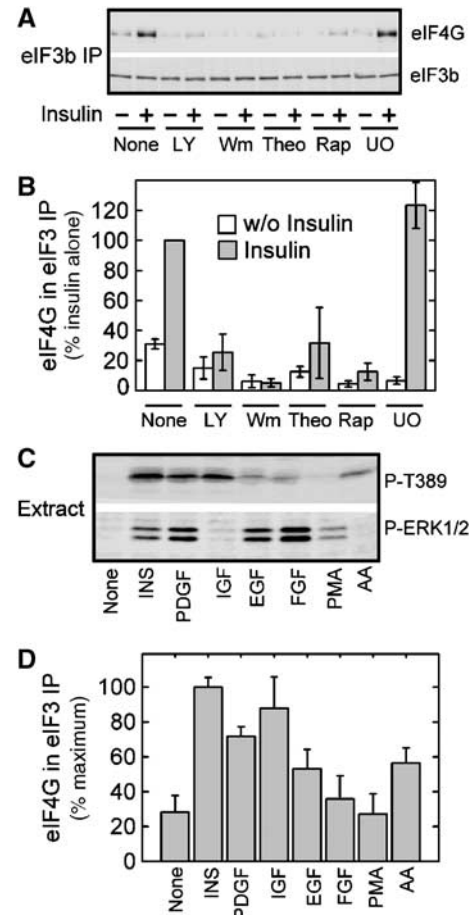


**Figure 8** Effects of inhibitors and activators of PI 3 kinase, mTOR, and MAP kinase signaling on the association of eIF3 and eIF4G. (A) Adipocytes were incubated without inhibitors (None) or with 50  $\mu$ M LY294002 (LY), 100 nM wortmannin (Wm), 5 mM theophylline (Theo), 20 nM rapamycin (Rap), or 20  $\mu$ M U0126 (UO). After adding insulin (10 mU/ml) as indicated, the incubations were continued for 15 min. Immunoblots were prepared to detect eIF4G and eIF3b in immune complexes isolated using eIF3b antibodies. (B) The amounts of eIF4G coimmunoprecipitating with eIF3 were expressed relative to the eIF4G recovered from cells that had been incubated with insulin alone. Mean values  $\pm$  s.e. of three experiments are presented. (C, D) Adipocytes were incubated for 5 min at 37°C without additions (None) or with 10 mU/ml insulin (INS), 5 nM platelet-derived growth factor BB (PDGF), 5 nM insulin-like growth factor 1 (IGF), 5 nM epidermal growth factor (EGF), 5 nM fibroblast growth factor 1 (FGF), 100 nM phorbol 12-myristate 13-acetate (PMA), or 2  $\times$  MEM amino acids plus 0.5 mM L-leucine (AA). (C) Immunoblots were prepared using phosphospecific antibodies to the T389 site in S6K1 or the activating sites in ERK1 and ERK2. (D) The relative amounts of eIF4G coimmunoprecipitating with eIF3 were expressed as percentages of the maximum recovered. Mean values  $\pm$  s.e. of three experiments are presented.

increasing eIF4G binding to eIF3. In contrast, IGF-1 did not activate MAP kinase, but it was equally effective as insulin in increasing eIF3–eIF4G (Figure 8C). These results with IGF-1 and FGF-1, and the failure of U0126 to block the effect of insulin (Figure 8B), indicate that activation of MAP kinase is neither necessary nor sufficient for increasing eIF4G binding to eIF3.

**Discussion**

Our results indicate that both physical and functional links exist between mTOR and eIF3. The finding that mTOR is able

to associate with eIF3f adds to the evidence of a physical association between eIF3 and mTOR very recently described (Holz *et al*, 2005). The role of the eIF3f within the eIF3 complex has not been defined. eIF3f is not found in *S. cerevisiae*; however, in *Schizosaccharomyces pombe* eIF3f is essential for viability, and depleting eIF3f markedly decreases global protein synthesis in fission yeast (Zhou *et al*, 2005). eIF3f is one of two eIF3 subunits that contain an MPN (Mpr1/Pad1 N-terminal) motif, which is found in certain subunits in two macromolecular complexes that are homologous to eIF3—the COP9 signalosome and the lid of the 19S proteasome (Hofmann and Bucher, 1998). Whether mTOR is targeted to these other two complexes is unknown; however, the association with eIF3 places mTOR in a prime position to control the interactions between eIF3 and other initiation factors. The rapamycin-sensitive effect of insulin on increasing the association of eIF3 and eIF4G represents a novel functional link between mTOR and eIF3.

How mTOR controls the association of eIF4G–eIF3 is still unclear, and there are many potential targets. Since many of the effects of mTOR are known to involve changes in protein phosphorylation, the association of mTOR with eIF3 suggested that phosphorylation of eIF3 subunits might be involved. eIF3b phosphorylation has been reported to be stimulated by insulin (Morley and Traugh, 1990). eIF3i, also known as TRIP-1, associates with and is phosphorylated by the type 2 TGF- $\beta$  receptor (Chen *et al*, 1995). Interestingly, the COOH terminal sequence in eIF3i (FEFEF), and a sequence in eIF3c (FELDL), fit the consensus for a TOS motif, suggesting that these subunits might interact with the raptor subunit of mTORC1. However, we did not detect any effect of insulin or rapamycin on the phosphorylation of eIF3b or eIF3i in  $^{32}\text{P}$ -labeled 3T3-L1 adipocytes (results not shown).

Changes in the composition of eIF3 represent another potential mechanism for controlling eIF3 function. The amount of eIF3j in eIF3 influences the amount of 40S subunit associated with eIF3 (Miyamoto *et al*, 2005). Interestingly, treating cells with PMA for 24 h decreased the amount of eIF3j in eIF3, thus decreasing the amount of the 43S pre-initiation complex (Miyamoto *et al*, 2005). This particular response occurred much too slowly to account for the rapid effects of insulin on eIF3 and eIF4G association, and acute treatment of adipocytes with PMA did not change the amount of eIF4G bound to eIF3 (Figure 8D). Furthermore, we observed no effect of insulin on the eIF3j content of eIF3 in 3T3-L1 adipocytes (Supplementary Figure S2). The amount of rpS6 that coimmunoprecipitated with eIF3 (Figure 5B) was also unchanged by insulin, indicating that the association of eIF3 with the 40S ribosomal subunit was not acutely controlled by the hormone. Moreover, the findings that the effect of insulin on eIF3–eIF4G was retained after separating the factors from 40S ribosomes, both by high salt extraction and sucrose gradient centrifugation, indicates that the insulin response does not depend on eIF3 binding to ribosomes.

eIF4G is known to be a target of mTOR signaling (Raught *et al*, 2000). Ser1108, S1148, and S1192 in the COOH terminal domain of eIF4G are phosphorylated in a rapamycin-sensitive manner in cells, although the effect on eIF4G function is unknown. As an index of eIF4G phosphorylation, we monitored phosphorylation of the S1108 site by using a phospho-specific antibody. Insulin stimulated phosphorylation of this site, but this effect lagged behind the stimulatory effect on

eIF4G–eIF3. In addition, the S1108 site could be completely dephosphorylated by PP1<sub>C</sub> without affecting the amount of eIF4G bound to eIF3 (Supplementary Figure S1). Thus, it seems clear that phosphorylation of S1108 does not mediate the effect of insulin on the association of eIF3 and eIF4G. Our results do not exclude a role of phosphorylation of other sites, such as the two new sites identified in this study (Figure 2B).

The binding site for eIF4E is located in the NH<sub>2</sub> terminal third of eIF4G. X-ray crystallographic studies indicate that the binding of eIF4E results in a dramatic conformational change in eIF4G as it wraps around the NH<sub>2</sub> terminal region of eIF4E to form a molecular bracelet that increases the affinity of eIF4E for the mRNA cap (Gross *et al*, 2003). The possibility was considered that this major structural change increased the affinity of eIF4G for eIF3, thereby explaining the increase eIF4G bound to eIF3. However, this mechanism was eliminated by the finding that the insulin response was not compromised by introducing mutations into eIF4G that abolished high affinity binding to eIF4E.

The central domain of eIF4G contains binding sites for both eIF3 and eIF4A (Gingras *et al*, 1999; Keiper *et al*, 1999). Since these two factors bind eIF4G in a cooperative manner *in vitro* (Korneeva *et al*, 2000), an increase in eIF4A bound to eIF4G could lead to increased binding of eIF3. This is an unlikely explanation of the present results, since insulin did not change the amount of eIF4A bound to eIF4G (Figure 2C). The central third of eIF4G also contains an RNA-binding motif, which is required for internal initiation at certain IRES elements. Increasing eIF4G association with eIF3 would presumably facilitate translation of messages containing these elements.

Insulin decreased the amount of eIF4B associated with eIF3, but in a rapamycin-insensitive manner (Figure 6). This response was first detected by silver staining and identification of the eIF4B protein by mass spectrometric sequencing, and it was subsequently confirmed by immunoblotting. Curiously, Holz *et al* (2005) found that insulin increased eIF4B associated with eIF3, and that overexpressing eIF4B stimulated cap-dependent translation, an effect opposite to that observed by others (Milburn *et al*, 1990; Raught *et al*, 2004). The reason for the differences in eIF4B responses among laboratories is unclear. However, it is unlikely that the rapid increase in eIF4G–eIF3 association produced by insulin occurred secondarily to changes in eIF4B binding to eIF3, since the effects on eIF4B in our experiments and those of Holz *et al* (2005) occurred relatively late in the insulin time course.

Although further research will be needed to determine the mechanism, we believe that the present evidence of mTOR association with eIF3, and the discovery that mTOR controls the association of eIF3 and eIF4G, provide important insight into the mechanisms of mTOR signaling and the control of protein synthesis by insulin and certain growth factors. By increasing 4EBP1 phosphorylation via mTOR signaling, insulin promotes eIF4E binding to eIF4G, thus increasing eIF4F bound to the 5' cap region of the mRNA (Gingras *et al*, 1999; Harris and Lawrence, 2003). Stimulating eIF4G binding to eIF3 would be expected to enhance joining of the eIF4F and the 40S ribosome, thus increasing the rate at which the small ribosomal subunit is positioned on the mRNA to begin scanning.



## Materials and methods

Descriptions of the yeast two-hybrid screen, preparation of viruses and plasmids, purification of recombinant proteins, sucrose gradient centrifugation, and mass spectrometric analyses have been included in Supplementary data.

### Antibodies

Antibodies to eIF4E and the phosphospecific antibodies to the T36/45 and S64 sites in 4EBP1 were the same as previously described (Mothe-Satney *et al*, 2000). The antibodies to eIF3a (L-18), eIF3b (N-20), and eIF3j (C20) were from Santa Cruz. Antibodies to ribosomal protein S6 (rpS6) and phosphospecific antibodies to sites in S6K1, Akt2, eIF4B, eIF4G, and the activating sites in ERK1 and ERK2 were from Cell Signaling. The antibody to eIF3i was provided by Rik Derynck (University of California San Francisco). Monoclonal antibody to the HA epitope tag was purified from 12CA5 hybridoma culture medium. FLAG antibodies were from Sigma-Aldrich.

To generate eIF4G and eIF4A antibodies, peptides having NH<sub>2</sub> terminal C followed by sequences identical to positions 517–535 (KRRRKIKELNKKKEAVGDLL) in mouse eIF4G-1 and positions 376–395 (VTEEDKRTLRLDIETFYNTSI) in mouse eIF4A-1 were coupled to keyhole limpet hemocyanin, and the peptide–hemocyanin conjugates were used to immunize rabbits. Antibodies were purified using columns containing affinity resins prepared by coupling the respective peptides to Sulfolink beads (Pierce).

### Cell culture and incubations

293T cells were cultured and transfected with 10 µg of expression plasmid per 10-cm dish using Lipofectamine 2000 (Invitrogen), and cultured essentially as described previously (McMahon *et al*, 2002). Mouse 3T3-L1 fibroblasts (ATCC # CL-173) were differentiated into adipocytes by culturing in growth medium as described previously (Lin *et al*, 1995). To initiate experiments, 293T cells or adipocytes (9–12 days postdifferentiation) were rinsed and incubated for 2 h at 37°C in Buffer A (145 mM NaCl, 5.4 mM KCl, 1.4 mM CaCl<sub>2</sub>, 1.4 mM MgSO<sub>4</sub>, 25 mM NaHCO<sub>3</sub>, 5 mM glucose, 5 mg/ml bovine serum albumin, 0.2 mM sodium phosphate and 10 mM HEPES, pH 7.4). Cells were then incubated with additions for the times indicated.

Incubations were terminated by rinsing cells twice with chilled PBS and immediately homogenizing the cells (1 ml buffer per 10 cm dish) by using a Teflon-glass tissue grinder. The homogenization buffer contained Buffer B (50 mM NaF, 1 mM EDTA, 1 mM EGTA, 0.1% Tween-20, 10 mM sodium phosphate, and 50 mM β-glycerophosphate, pH 7.4) supplemented with 1 mM phenylmethylsulfonyl fluoride, 10 µg/ml leupeptin, 10 µg/ml aprotinin, 10 µg/ml pepstatin, and 0.5 µM microcystin. Homogenates were centrifuged at 10 000g for 20 min, and the supernatants were retained for analyses.

### GST pulldowns

GST-CTmTOR (2 µg) or GST-eIF3f (2 µg) were incubated with 15 µl of packed GSH-Sepharose beads in Buffer B for 1 h, and then washed with 1 ml of Buffer B. Lysates from 293T cells (750 µl) were added to the beads and the samples were incubated at 4°C for 15 h with constant mixing. The beads were washed four times with 1 ml Buffer B and eluted using SDS sample buffer.

## References

- Abraham RT, Wiederricht GJ (1996) Immunopharmacology of rapamycin. *Ann Rev Immunol* **14**: 483–510
- Asano K, Phan L, Anderson J, Hinnebusch AG (1998) Complex formation by all five homologues of mammalian translation initiation factor 3 subunits from yeast *Saccharomyces cerevisiae*. *J Biol Chem* **273**: 18573–18585
- Bandyopadhyay A, Maitra U (1999) Cloning and characterization of the p42 subunit of mammalian translation initiation factor 3 (eIF3): demonstration that eIF3 interacts with eIF5 in mammalian cells. *Nucleic Acids Res* **27**: 1331–1337
- Browning KS, Gallie DR, Hershey JW, Hinnebusch AG, Maitra U, Merrick WC, Norbury C (2001) Unified nomenclature for the subunits of eukaryotic initiation factor 3. *Trends Biochem Sci* **26**: 284

### Immunoprecipitations

Extracts were passed through a 0.45 µm syringe filter before samples (750 µl) were incubated with 7.5 µl of packed protein G agarose beads to which 2 µg of antibodies had been bound. Nonimmune antibodies from goat or rabbit sera, respectively, were used as controls for specificity. After incubating at 4°C for 15 h with constant mixing, the beads were washed four times with Buffer B (1 ml/wash). Proteins were eluted by using SDS sample buffer.

### Affinity-purification of eIF4E complexes with m<sup>7</sup>GTP-agarose

eIF4E was partially purified by using m<sup>7</sup>GTP-Sepharose 4B (GE Healthcare). Extract samples (750 µl) were mixed with 20 µl of m<sup>7</sup>GTP-Sepharose 4B for 1 h at 21°C. The beads were washed four times with Buffer B (1 ml/wash) before proteins were eluted with SDS sample buffer.

### Electrophoretic analyses

Samples were subjected to electrophoresis in the presence of SDS in 8.75% polyacrylamide gels (Laemmli, 1970). Proteins were detected with a silver staining kit following the instructions provided by the supplier (Bio-Rad) or with Coomassie blue as described previously (Huffman *et al*, 2002). For immunoblotting, proteins were electrophoretically transferred to 0.45 µm PVDF membranes (Immobilon-P, Millipore). The membranes were blocked by incubating in 10% dried milk in Buffer C (150 mM NaCl, 2% Tween-20, and 50 mM Tris-HCl, pH 7.4) for at least 1 h. Membranes were then incubated with primary antibodies (0.5 µg/ml) for 2 h in Buffer C containing 0.1% milk, washed four times (1 ml/wash) with Buffer C, and then incubated with the appropriate secondary antibodies conjugated to alkaline phosphatase for 1 h. After washing membranes four times with Buffer C, the secondary antibodies bound were detected by using CDP-Star reagent (Tropix) and either a Fujifilm LAS 3000 LCD camera or film (Kodak X-Omat AR). Films were analyzed by using a scanning laser densitometer. Relative band intensities were determined by using the volume integration function of the ImageQuant 5.2 program (Molecular Dynamics).

### Other materials

Rapamycin, FK506, LY294002, and U0126 were purchased from Calbiochem-Novabiochem International. Theophylline, IGF-1 and wortmannin were from Sigma-Aldrich. Tween-20 was from Fischer Scientific. EGF was from Upstate Biologicals. FGF1 was provided by Dr David Ornitz (Washington University). Insulin (Novolin R) was from Novo Nordisk. PDGF-BB was from Cell-Signaling. The plasmid, pRK70-HA-p70S6K, for overexpressing HA-S6K1 was provided by John Blenis. Recombinant PP1<sub>C</sub> was generously provided by Anna DePaoli-Roach (Indiana University).

### Supplementary data

Supplementary data are available at *The EMBO Journal* Online.

## Acknowledgements

This research was supported in part by NIH Grants DK52753 and DK28312 to JCL, GM 37537 to DFH, and GM20818 to RER. We acknowledge the technical contributions of Sachin Nagrani and the assistance of Carrie Belfield in the yeast two-hybrid screens.

- Brunn GJ, Williams J, Sabers C, Wiederricht G, Lawrence JC, Abraham RT (1996) Direct inhibition of the signaling functions of the mammalian target of rapamycin by the phosphoinositide 3-kinase inhibitors, wortmannin and LY294002. *EMBO J* **15**: 5256–5267
- Chen RH, Miettinen PJ, Maruoka EM, Choy L, Derynck R (1995) A WD-domain protein that is associated with and phosphorylated by the type II TGF-beta receptor. *Nature* **377**: 548–552
- Gingras A-C, Raught B, Sonenberg N (1999) eIF4 initiation factors: effectors of mRNA recruitment to ribosomes and regulators of translation. *Ann Rev Biochem* **68**: 913–963
- Gross JD, Moerke NJ, von der Haar T, Lugovskoy AA, Sachs AB, McCarthy JE, Wagner G (2003) Ribosome loading onto the mRNA cap is driven by conformational coupling between eIF4G and eIF4E. *Cell* **115**: 739–750

- Harris TE, Lawrence JC (2003) TOR signaling. *Sci STKE* **2003**: re15
- Helentjaris T, Ehrenfeld E (1978) Control of protein synthesis in extracts from poliovirus-infected cells. I. mRNA discrimination by crude initiation factors. *J Virol* **26**: 510–521
- Hershey JW, Merrick WC (2000) The pathway and mechanism of initiation of protein synthesis. In *Translational Control of Gene Expression*, Sonenberg N, Hershey JW, Matthews MB (eds) pp 33–88. Cold Spring Harbor: Cold Spring Harbor Laboratory Press
- Hofmann K, Bucher P (1998) The PCI domain: a common theme in three multiprotein complexes. *Trends Biochem Sci* **23**: 204–205
- Holz MK, Ballif BA, Gygi SP, Blenis J (2005) mTOR and S6K1 mediate assembly of the translation preinitiation complex through dynamic protein interchange and ordered phosphorylation events. *Cell* **123**: 569–580
- Huffman TA, Mothe-Satney I, Lawrence JC (2002) Insulin-stimulated phosphorylation of lipin mediated by the mammalian target of rapamycin. *Proc Natl Acad Sci USA* **99**: 1047–1052
- Keiper BD, Gan W, Rhoads RE (1999) Protein synthesis initiation factor 4G. *Int J Biochem Cell Biol* **31**: 37–41
- Kimball SR, Vary TC, Jefferson LS (1994) Regulation of protein synthesis by insulin. *Ann Rev Physiol* **56**: 321–348
- Korneeva NL, Lamphear BJ, Hennigan FL, Rhoads RE (2000) Mutually cooperative binding of eukaryotic translation initiation factor (eIF) 3 and eIF4A to human eIF4G-1. *J Biol Chem* **275**: 41369–41376
- Laemmli UK (1970) Cleavage of structural proteins during the assembly of the head of bacteriophage T4. *Nature* **227**: 680–685
- Lin T-A, Kong X, Saltiel AR, Blackshear PJ, Lawrence JC (1995) Control of PHAS-I by insulin in 3T3-L1 adipocytes: synthesis, degradation, and phosphorylation by a rapamycin-sensitive and MAP kinase-independent pathway. *J Biol Chem* **270**: 18531–18538
- Lin T-A, Lawrence JC (1997) Control of PHAS-I phosphorylation in 3T3-L1 adipocytes: effects of inhibiting protein phosphatases and the p70S6K signalling pathway. *Diabetologia* **40** (Suppl 2): S18–S24
- Mader S, Lee H, Pause A, Sonenberg N (1995) The translation initiation factor eIF-4E binds to a common motif shared by the translation factor eIF-4G and the translational repressor 4E-binding proteins. *Mol Cell Biol* **15**: 4990–4997
- Martin DE, Hall MN (2005) The expanding TOR signaling network. *Curr Opin Cell Biol* **17**: 158–166
- McMahon LP, Choi KM, Lin T-A, Abraham RT, Lawrence JC (2002) The rapamycin-binding domain governs substrate selectivity by the mammalian target of rapamycin. *Mol Cell Biol* **22**: 7428–7438
- Milburn SC, Hershey JW, Davies MV, Kelleher K, Kaufman RJ (1990) Cloning and expression of eukaryotic initiation factor 4B cDNA: sequence determination identifies a common RNA recognition motif. *EMBO J* **9**: 2783–2790
- Miyamoto S, Patel P, Hershey JW (2005) Changes in ribosomal binding activity of eIF3 correlate with increased translation rates during activation of T lymphocytes. *J Biol Chem* **280**: 28251–28264
- Morley SJ, Traugh JA (1990) Differential stimulation of phosphorylation of initiation factors eIF-4F, eIF-4B, eIF-3, and ribosomal protein S6 by insulin and phorbol esters. *J Biol Chem* **265**: 10611–10616
- Mothe-Satney I, Brunn GJ, McMahon LP, Capaldo CT, Abraham RT, Lawrence JC (2000) Mammalian target of rapamycin-dependent phosphorylation of PHAS-I in four (S/T)P sites detected by phospho-specific antibodies. *J Biol Chem* **275**: 33836–33843
- Nojima H, Tokunaga C, Eguchi S, Oshiro N, Hidayat S, Yoshino K, Hara K, Tanaka N, Avruch J, Yonezawa K (2003) The mammalian target of rapamycin (mTOR) partner, raptor, binds the mTOR substrates p70 S6 kinase and 4E-BP1 through their TOR signaling (TOS) motif. *J Biol Chem* **278**: 15461–15464
- Nygard O, Westermann P (1982) Specific interaction of one subunit of eukaryotic initiation factor eIF-3 with 18S ribosomal RNA within the binary complex, eIF-3 small ribosomal subunit, as shown by cross-linking experiments. *Nucleic Acids Res* **10**: 1327–1334
- Phan L, Zhang X, Asano K, Anderson J, Vornlocher HP, Greenberg JR, Qin J, Hinnebusch AG (1998) Identification of a translation initiation factor 3 (eIF3) core complex, conserved in yeast and mammals, that interacts with eIF5. *Mol Cell Biol* **18**: 4935–4946
- Preiss T, Hentze MW (2003) Starting the protein synthesis machine: eukaryotic translation initiation. *Bioessays* **25**: 1201–1211
- Raught B, Gingras AC, Gygi SP, Imataka H, Morino S, Gradi A, Aebersold R, Sonenberg N (2000) Serum-stimulated, rapamycin-sensitive phosphorylation sites in the eukaryotic translation initiation factor 4GI. *EMBO J* **19**: 434–444
- Raught B, Peiretti F, Gingras A-C, Livingstone M, Shahbazian D, Mayeur GL, Polakiewicz RD, Sonenberg N, Hershey JW (2004) Phosphorylation of eucaryotic translation initiation factor 4B Ser422 is modulated by S6 kinases. *EMBO J* **23**: 1761–1769
- Sarbasov DD, Ali SM, Sabatini DM (2005) Growing roles for the mTOR pathway. *Curr Opin Cell Biol* **17**: 596–603
- Schalm SS, Fingar DC, Sabatini DM, Blenis J (2003) TOS motif-mediated raptor binding regulates 4E-BP1 multisite phosphorylation and function. *Curr Biol* **13**: 797–806
- Simpson IA, Cushman SW (1986) Hormonal regulation of mammalian glucose transport. *Ann Rev Biochem* **55**: 1059–1089
- Vornlocher HP, Hanachi P, Ribeiro S, Hershey JW (1999) A 110-kilodalton subunit of translation initiation factor eIF3 and an associated 135-kilodalton protein are encoded by the *Saccharomyces cerevisiae* TIF32 and TIF31 genes. *J Biol Chem* **274**: 16802–16812
- Zhou C, Arslan F, Wee S, Krishnan S, Ivanov AR, Oliva A, Leatherwood J, Wolf DA (2005) PCI proteins eIF3e and eIF3m define distinct translation initiation factor 3 complexes. *BMC Biol* **3**: 14